ENGINEERING

Supramolecular silicone coating capable of strong substrate bonding, readily damage healing, and easy oil sliding

Meijin Liu[1], Zhaoyue Wang[1], Peng Liu[1], Zuankai Wang[2], Haimin Yao[3], Xi Yao[1,4]*

Polymer coatings with a combined competence of strong bonding to diverse substrates, broad liquid repellency, and readily damage healing are in substantial demand in a range of applications. In this work, we develop damage-healable, oil-repellent supramolecular silicone (DOSS) coatings to harvest abovementioned properties by molecular engineering siloxane oligomers that can self-assemble onto coated substrates via multivalent hydrogen bonding. In addition to the readily damage-healing properties provided by reversible association/dissociation of hydrogen bonding motifs, the unique molecular configuration of the siloxane oligomers on coated substrates enables both robust repellency to organic liquids and strong bonding to various substrates including metals, plastics, and even Teflon. We envision that not only DOSS coatings can be applied in a range of energy, environmental, and biomedical applications that require long-term services in harsh environmental conditions but also the design strategy of the oligomers can be adopted in the development of supramolecular materials with desirable multifunctionality.

INTRODUCTION

Liquid-repellent surfaces that repel low–surface tension liquids have been extensively studied because of their promising applications in self-cleaning (*1*–*3*), antifouling (*4*, *5*), flexible electronics (*6*), catalysis (*7*, *8*), and heat transfer (*9*). In practice, these coatings are commonly required to firmly adhere to various substrates, are transparent, and are persistent to harsh conditions [such as ultraviolet (UV) irradiation and heat] and mechanical damages (*2*, *10*). Although individual features have been realized in various materials, it remains a major challenge to fulfill all the requirements without compromising each other. For example, self-healable superhydrophobic (*11*) and superoleophobic (*12*) polymer coatings have been reported to recover from plasma-induced chemical damages, but they are not tolerant to mechanical damages when the sophisticated microstructure is destroyed. Incorporation of perfluorooctanoate (PFO) anions onto layer-by-layer deposited polymer films could also provide healable coatings with low oil sliding angles (*13*). Despite the complicated fabrication procedure and elusive interfacial bonding properties, the use of PFO will also raise concerns on health and environmental impact (*14*). Slippery liquid-infused porous surfaces (SLIPS) show improved damage tolerance (*15*) with the help of lubricant reconfiguration on the porous substrates; however, these healing mechanisms cannot fully solve the issues of physical damages on solid substrates (*16*, *17*). Recently, there are a couple of supramolecular organogels showing persistent self-healing and water-sliding properties under multiple scratches (*18*, *19*) because the damaged surface becomes flat after healing, which would facilitate the restoration of surface slipperiness. However, their molecular design does not allow them to repel common hydrocarbon solvents, which will severely affect the lubricating oils that serve as lubricating layer. Furthermore, the lubricating oil on the organogel surface would also largely reduce the interfacial adhesion onto the coated substrates (*20*). To address these issues and challenges, a holistic consideration of the molecular engineering of the coating material is highly desired.

Silicone-based polymers and elastomers containing polydimethylsiloxane (PDMS) backbones are responsible for waterproof properties, chemical resistance, biocompatibility, and ease of material integration for multifunctionality (*8*, *21*, *22*). Recently, by taking the advantages of supramolecular chemistry (*23*, *24*) in regulating mechanical integrity through reversible cross-linking (*25*–*27*), people have developed silicone-based supramolecular materials with unique features of intrinsic healing, stimuli responsiveness, flexibility, elasticity, and toughness (*28*). These properties make them promising candidates in the emerging and developed fields, such as artificial skin (*29*), soft robotics (*30*), and advanced coating applications (*18*–*20*). However, in accordance with coating applications, current supramolecular silicones lack satisfactory stiffness and mechanical strength, their bonding capacity on various substrates has not been well studied, and the effect of incorporated chemical motifs that provide dynamic bonding on liquid repellency remains unknown.

We here report the development of damage-healable, oil-repellent supramolecular silicone (DOSS) coatings harvesting a combination of features that have been rarely reported including broad liquid repellency to various alkyl oils, high mechanical strength and strong adhesion to diverse surfaces, reliable damage healing, and ease of manufacturing. The DOSS coatings are prepared by molecular engineering telechelic siloxane oligomers, which have functional groups as the end groups and can self-assemble onto various substrates to form a large-scale network via multivalent hydrogen bonding. The synthesized siloxane oligomer has a unique three-arm design with a trifunctional center and a terminal 2-amino-4-hydroxy-6-methylpyrimidine (UPy) motif and a siloxane backbone on each arm (Fig. 1). Compared to linear polymers, these oligomers could offer higher cross-linking density when self-assembled into large-scale networks and thus a DOSS coating, which would globally benefit the surface and mechanical properties of the obtained coating. Furthermore, complementary hydrogen bonding provided by the UPy motifs could

[1]Department of Biomedical Sciences, City University of Hong Kong, 83 Tat Chee Avenue, Kowloon, Hong Kong, P. R. China. [2]Department of Mechanical Engineering, City University of Hong Kong, 83 Tat Chee Avenue, Kowloon, Hong Kong, P. R. China. [3]Department of Mechanical Engineering, The Hong Kong Polytechnic University, Hung Hom, Kowloon, Hong Kong, P. R. China. [4]Shenzhen Research Institute of City University of Hong Kong, Shenzhen 518075, P. R. China.
*Corresponding author. Email: xi.yao@cityu.edu.hk

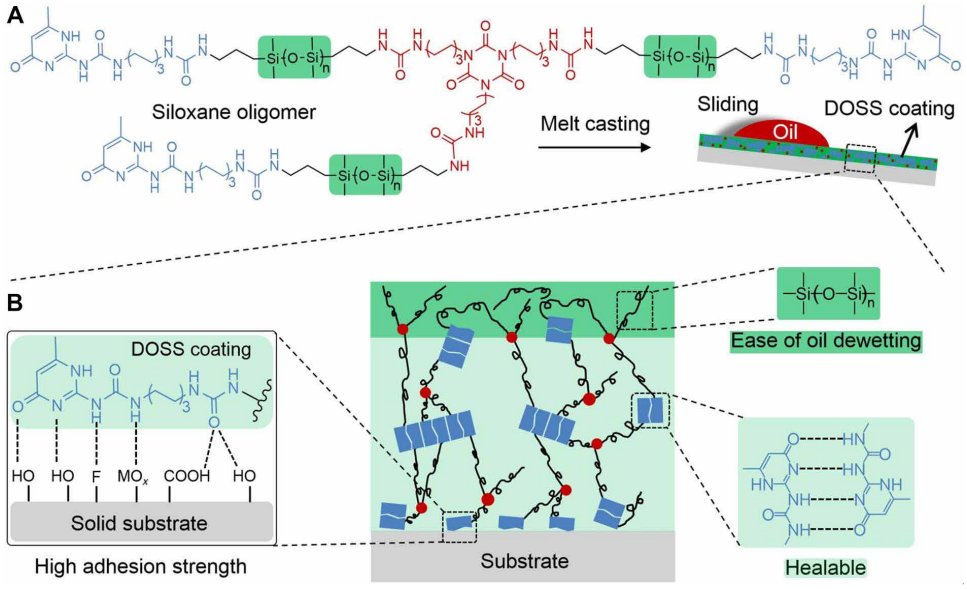

Fig. 1. Schematic illustration of the preparation of the healable DOSS coatings. (**A**) Chemical structure of three-arm siloxane oligomer and preparation of the DOSS coating with small oil slide angles. The coatings are prepared by melting siloxane oligomer grind and then casting them onto the substrate. (**B**) Structure of the DOSS coating on a substrate. The PDMS domains enriched in the surface of the DOSS coating offer the properties of oil sliding and dewetting; the multiple hydrogen bonds in the interior of the DOSS coating make it healable. The strong interaction between the DOSS coating and the substrate through hydrogen bonding enables the coating to firmly adhere to various substrates.

enhance the damage-healing and mechanical properties of the coating (*31*); the siloxane motifs at suitable molecular weights (MWs) would facilitate the dewetting of impinging oils and thus contribute to oil repellency, and the high-density UPy motifs at the coating/substrate boundary also contribute to strong interfacial adhesion due to the intensive hydrogen bonding (*32*). The correlation between the molecular architecture and coating properties is revealed.

RESULTS

Preparation and characterizations

The synthesis method of the siloxane oligomer has been reported in our previous work (*31*), and the synthesized siloxane oligomers are thermal-casted onto different substrates to form coatings with thickness of 15 to 360 μm. The MWs of siloxane backbones in the oligomers are tuned at ~870, ~3000, and ~5000 for comparison. It is found that the overall mechanical properties of the DOSS coatings decrease exponentially with the increase of the chain length of the siloxane backbones (fig. S1 and table S1), probably because the longer siloxane backbones in the oligomers would reduce the density of physical cross-linking points originated from the hydrogen-bonded UPy dimers and the microstructures in the interior of the coating (*33*). This is confirmed by powder x-ray diffraction—that the DOSS coatings with the siloxane backbone at ~870 MW are characteristic semicrystalline and the DOSS coatings with the siloxane backbones at ~3000 and ~5000 MW are amorphous (figs. S1 and S2). Therefore, coatings prepared from siloxane oligomers with ~870-MW siloxane backbones are used as typical samples in most characterization tests.

The molecular configuration of the DOSS coating casted on bare glass slides is first studied via attenuated total reflectance infrared (ATR-IR), x-ray photoelectron spectroscopy (XPS), and atomic force microscopy (AFM). The top surface layer of the coating is examined directly, and the coating is peeled from the glass slide to expose the bottom layer at the coating/substrate interface and sectioned to expose the interior layer inside the coating, respectively. Higher relative intensity of the peak assigned to siloxane groups and higher silicon atom content in the surface layer (Fig. 2A, figs. S3 to S6, and tables S2 and S3) are observed in ATR-IR and XPS spectra, implying that the siloxane motifs are enriched in the surface layer of the DOSS coating. Furthermore, the ATR-IR spectra also reveal that there are abundant dissociated UPy motifs in the bottom layer at the coating/glass interface (*34*). In contrast, most UPy motifs are in the form of associated dimers and stacks in the interior of the coating, and both associated and dissociated UPy motifs exist in the surface layer of the coating, respectively. Therefore, AFM measurements on the adhesion forces of each layer are subsequently performed (*31*, *35*), and an area of 9 μm × 9 μm is scanned with 256 × 256 test points to acquire the mapping and averaged adhesion forces of each sample (Fig. 2, B to G, and fig. S7). The average adhesion force of the bottom layer is 8.3 nN, which is higher than that in the interior (6.9 nN) and in the surface layer (0.31 nN). The sharp increase on the adhesion force from the surface layer to the bottom layer correlates very well with the distribution of the dissociated UPy motifs and the siloxane backbones in the two layers. There are more dissociated UPy motifs and less siloxane backbones in the bottom layer, which is favorable to the strong bonding capability at the coating/substrate interface, and there are less UPy motifs and more siloxane backbones in the surface layer, which is expected to facilitate the dewetting of oils on the surface of the coating (*36*–*40*).

Adhesive properties

The adhesion strength on various substrates is subsequently evaluated. The siloxane oligomers are deposited on a glass slide and processed by heating to produce a uniform film with a thickness of ca. 0.2 mm.

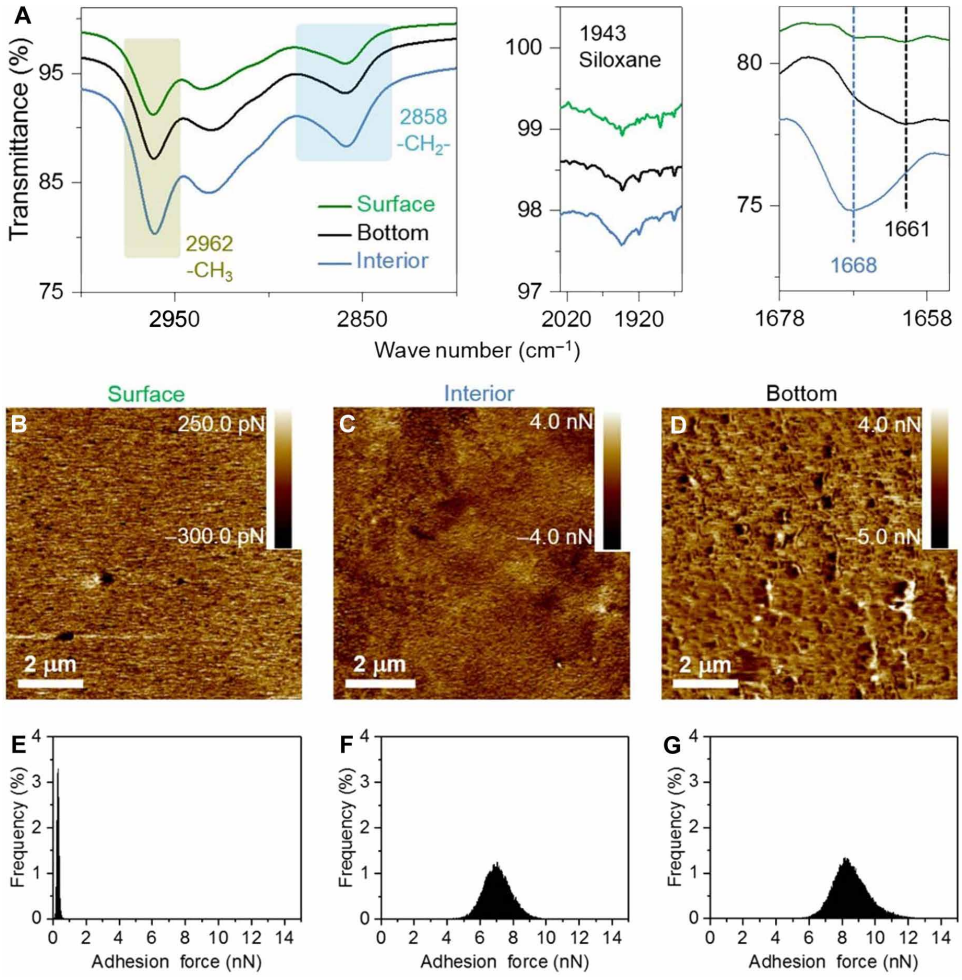

Fig. 2. Molecular configuration and adhesion force analyses of DOSS coatings. (**A**) ATR-IR spectra showing the comparison intensities of featured groups in the surface layer (green line), interior section (blue line), and bottom layer (black line) of the DOSS coating adhered on a substrate. The two colored boxes indicate peaks of methyl group (light yellow) and methylene group (light blue), respectively. Dashed lines indicate peaks regarding UPy motifs in aggregated state (blue) and dissociated state (black), respectively. (**B** to **D**) AFM adhesion force images (9 μm × 9 μm) of the surface layer, interior section, and bottom layer of the DOSS coating. (**E** to **G**) Distributions of adhesion forces measured between the bare AFM tip and the surface layer, interior section, and bottom layer of the DOSS coating. The adhesion force increases sequentially from the surface layer (B and E), to the interior section (C and F), and to the bottom layer (D and G) of the DOSS coating.

Then, another glass plate is pressed on that adhesive layer. Subsequent cooling to room temperature (25°C) for 10 min enabled the reformation of the siloxane oligomer network between the two glass slides, resulting in uniform contact and firm bonding. A weight of 1 kg can be hung up under the two adhered glass slides with a glued area of 1 cm^2, and the siloxane oligomer-based adhesives work well on a variety of substrates including hydrophilic cellulose (paper), aluminum, copper, and hydrophobic Teflon following the same protocol (fig. S8). Quantitative tests show that a shear strength above 20 MPa is recorded (Fig. 3A) for cellulose (paper) and all tested metal substrates and about 10 MPa for Teflon, outstanding among the commercial glues and other adhesive materials that have ever been reported (*32*, *33*, *41*–*52*). This high shear strength can be ascribed to the high mechanical strength of the siloxane oligomers and the high-density H-bonds between the urea and UPy motifs, especially the dissociated UPy motifs at the DOSS coatings/substrate interface, which can form hydrogen bonding with either the hydroxyl groups of hydrophilic surfaces or the fluorine groups of the hydrophobic Teflon surface (Fig. 3B, fig. S3, and table S2). The high mechanical strength and the strong adhesion strength over a variety of substrates highlight the versatility of the siloxane oligomers as universal adhesives.

Oil-repellent and self-healing properties

The DOSS coatings are prepared on various substrates with little change to the appearance of the coated substrates due to the native transparency of the coating. By using *n*-hexadecane as a probing liquid, all the DOSS coatings on tuning substrates exhibit small contact angle hysteresis [CAH; i.e., difference between the advancing (θ_{Adv}) and receding (θ_{Rec})] (Fig. 4A). This is consistent with the reported results of polysiloxane-based coatings with easy oil sliding/dewetting properties (*36*–*40*). However, the CAH increases with the increase of the chain length of the siloxane backbone in the oligomers (fig. S9). That is, the coating prepared from oligomers with ~870-MW siloxane demonstrates lower CAH and better oil repellency than the coatings prepared from oligomers with ~3000- and ~5000-MW siloxane, although there is higher siloxane content in the surface layer of the

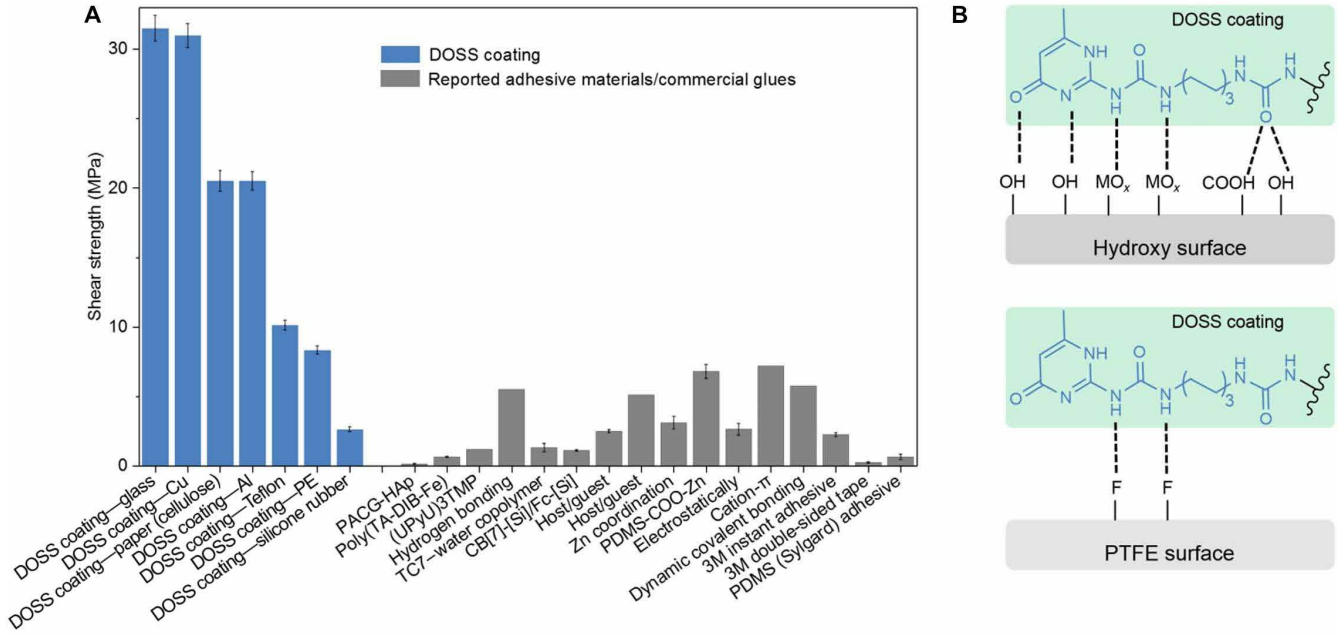

Fig. 3. Comparison of shear strengths between DOSS coatings and reported adhesive materials/commercial glues. (**A**) The shear strength between the DOSS coating and various substrates (blue columns) and, as a comparison, the results of reported adhesive materials/commercial glues (black columns) are listed (*32*, *33*, *41*–*52*). The shear strength reported in this work is competitive with the results of reported adhesive materials/commercial glues. (**B**) Schematic illustration of the strong interaction between the coating and the adhered substrate through hydrogen bonding. PTFE, polytetrafluoroethylene.

latter two DOSS coatings (figs S10 and S11 and table S4). SEM data show that there are denser microcracks on the surfaces of DOSS coatings prepared from oligomers with ~3000- and ~5000-MW siloxane (fig. S12), and these microcracks will serve as topography defects and affect CAHs (*53*), which explains well the CAH increase of the three coatings.

In further evaluation, nonpolar organic solvents, including *n*-hexane, *n*-octane, *n*-dodecane, *n*-hexadecane, and commercial edible oils (e.g., grape seed oil and olive oil), and polar organic solvents, such as alcohol (EtOH), ethyl ether, acetone, toluene, chloroform, tetrahydrofuran (THF), and dimethyl formamide (DMF) with various surface tensions (labeled below the *x* axis of Fig. 4, B and C), are taken as the probe liquids. All the nonpolar probe liquids exhibit CAH lower than 5° on the DOSS coatings, indicating the easy sliding/dewetting of the nonpolar liquids on top of the coatings. Note that the DOSS coatings can repel most commercial edible oils with high viscosity, assisting their potential values in daily life. Varying the coating thickness from 15 to 360 μm or exposing the coating upon continuous heat treatment and UV irradiation (365 nm and 5 mW/cm^2) for 30 days does not affect the CAH of the coating, indicating outstanding stability (fig. S13). In contrast, the coating shows increased CAH to a couple of tested polar organic liquids (Fig. 4C). The ease of oil dewetting to the nonpolar liquids on DOSS coatings could be ascribed to the weak interaction between the oil droplet and the siloxane-enriched surface where the UPy motifs on the surface layer are shielded by the siloxane motifs, while the high CAH of the DOSS coating to polar organic liquids indicates stronger interaction (*54*) of the solvent molecules with the surface layer of the coating. This is probably because the siloxane backbones are of better mobility in the polar organic solvents, which will expose the shielded UPy motifs and thus results in strong molecular interaction and high CAH (Fig. 4D) (*55*).

In addition to the abovementioned features, the as-prepared DOSS coating exhibits excellent damage-healing properties. To demonstrate the healing/recovery behavior, we probe the oil repellency of the coating by incorporating crosscutting lines to the coatings via a blade and subsequently monitoring the liquid sliding on the surfaces, as shown in Fig. 5. The *n*-hexadecane drop readily slides down the original surface of the DOSS coating casted on a glass slide (Fig. 5A). When the crosscut damage is introduced, the *n*-hexadecane drop is blocked and pinned at the damage region of the coating (Fig. 5, B and E). Subsequently, we remove the residual oil on the surface by blowing nitrogen gas for 20 s and heat the coating at 90°C for 15 min to facilitate the coating recovery (fig. S14). The crosscutting lines disappear accordingly after the treatment, and the oil drop slides smoothly on the healed surface (Fig. 5, C and F). We further study the durability of the oil repellency by measuring the recovery of the CAH during 30 cycles of cut and heal. It turns out that the repeated treatments will not affect the morphology and chemistry of the coating, implying excellent cyclic reproducibility and high reliability of the oil-repellent surface.

DISCUSSION

The highly ordered assembly of three-arm siloxane oligomers, as well as the configuration of the oligomer network on various substrates, provides an easy-to-use strategy for the fast fabrication of robust coatings featuring strong interfacial bonding, broad liquid repellency, and damage-healing properties. We investigated the structure of the assembled oligomers on the substrate systematically. It is interesting to find that the siloxane domains are enriched in the surface layer, while the UPy domains, especially the dissociated ones, are enriched in the bottom layer of the coatings. We revealed that the supramolecular assembly with high cross-linking densities plays synergistic roles in

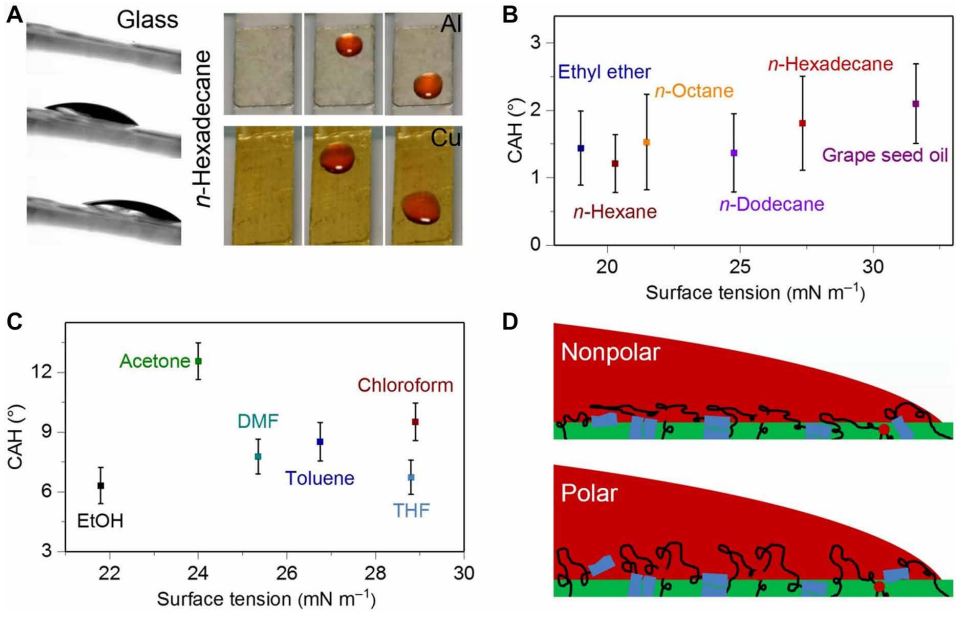

Fig. 4. Wettability of the DOSS coatings. (**A**) The siloxane oligomer material–based coatings with small oil slide angles can be applied to various substrates such as glass, Al, and Cu sheets, and 10-μl *n*-hexadecane drops can be repelled by all these coated surfaces. Credit: Meijin Liu, City University of Hong Kong. (**B** and **C**) CAH of various liquids on glass slides coated with siloxane oligomer materials. Nonpolar liquids can be repelled by the DOSS coating with a low CAH, while a couple of polar liquids can be repelled by the DOSS coating with a higher CAH. (**D**) Schematic illustrations of the interactions between the drops of nonpolar liquid or polar liquid and the DOSS coating, respectively. The interaction between the drop of nonpolar liquid and the DOSS coating is weak, as UPy motifs on the surface layer are shielded by the siloxane motifs, while the drop of polar liquid will strongly interact with the surface layer of the coating, particularly the dissociated UPy motifs, leading to higher CAHs.

the healable behaviors and mechanical properties of the coating, and the siloxane motifs enriched in the surface layer of the DOSS coating contribute to the robust oil repellency. Furthermore, the dense dissociated UPy motifs in the bottom layer facilitate strong interfacial bonding of the DOSS coating to a variety of substrates.

Different from traditional liquid-repellent surfaces such as superhydrophobic surfaces or SLIPS that demonstrate limited performances in damage healing and substrate bonding, the liquid-repellent coatings reported here are based on supramolecular polymers assembled from multiple hydrogen bonding. They can not only repel various alkyl oils but also exhibit reliable damage healing and strong adhesion with diverse surfaces, endowing them with great promise in a range of energy, environmental, and biomedical applications that require long-term services in harsh environmental conditions.

Furthermore, compared to linear polymers with an indefinite structure, these supramolecular polymers are more designable and manufacturable for multifunctionality because of the particularly oligomeric unit with a well-described structure. In addition, the UPy motif can be replaced with other hydrogen bonding suppliers such as catechol to incorporate multiple bonding mechanisms. The connector center can also be substituted with other molecules with specific geometry to tune the molecular assembly, and the MW of siloxane motifs can be tuned or other alternative polymer backbones can be selected to replace the siloxane motifs to adjust the mechanical and surface properties of the supramolecular materials. This strategy provides a new and powerful route to fabricate and engineer a wide range of supramolecular materials with desirable multifunctionalities. We envision that the results and insights obtained in this work can be applied in a wide variety of areas including self-cleaning, antifouling, catalysis, and heat transfer.

MATERIALS AND METHODS

Materials

PDMS bis(3-aminopropyl) terminated (H_2N-PDMS-NH_2; M_n = ~870, ~3000, and ~5000) was purchased from Gelest. UPy was purchased from Fisher Scientific (Acros Organics). Trifunctional homopolymer of hexamethylene diisocyanate was purchased from Bayer MaterialScience (Pittsburgh, PA, USA) and used as received. The other chemicals and solvents were purchased from Sigma-Aldrich. All chemicals were used as obtained, unless otherwise specified.

Methods

The optical images were obtained with an upright optical microscope (Nikon Eclipse Ni-U). Infrared spectra were recorded on a Fourier transform infrared spectrometer (PerkinElmer Spectrum Two, equipped with a Universal ATR sampling accessory and diamond crystal; PerkinElmer Instruments, The Netherlands). Transmission spectra were recorded at room temperature in the range from 4000 to 650 cm^{-1} at a resolution of 4 cm^{-1} and with an accumulation of 16 scans. A sample of free-standing siloxane oligomer film was placed on the crystal. To achieve good contact between the sample and the crystal, force was applied on top of the sample. The semicrystalline properties of the elastomers were examined under a polarizing optical microscope (Carl Zeiss microscope, Axioplan2 imaging) and an x-ray diffraction analysis instrument (Bruker AXS, D2 PHASER). Photographs of the membrane were taken using a digital camera (Nikon DSVR). The healing process was recorded with an upright optical microscope (Nikon Eclipse Ni-U). Mechanical tensile stress tests were performed using INSTRON-5566 based on the ASTM D2256 standard. For mechanical tensile stress tests, a sample size of 40 mm length × 5 mm width × 2 mm height, a gauge

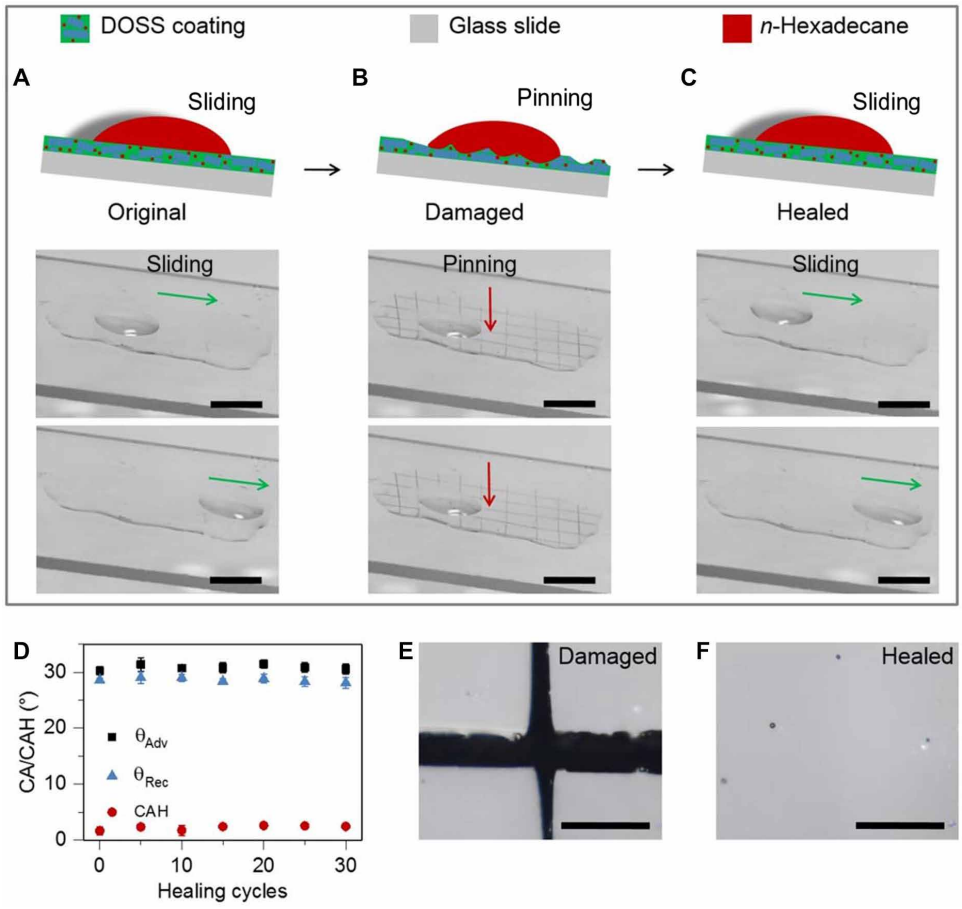

Fig. 5. Morphological and oil-repellent evaluation of self-healing coatings on glass slides. (**A**) A 10-μl *n*-hexadecane drop slides away on the pristine DOSS coating. (**B**) The DOSS coating is crosscut by a blade, and the 10-μl *n*-hexadecane drop is blocked at the damage region. (**C**) The damaged DOSS coating is treated by blowing nitrogen gas for 20 s and is subsequently healed by heating at 90°C for 15 min. A 10-μl *n*-hexadecane drop is repelled again on the healed surfaces, implying the recovery of oil repellency. (**D**) Repeating test on oil repellency of the coating after being damaged/healed for multiple cycles by using *n*-hexadecane as a probing liquid. (**E**) Optical microscopy image of a damaged film. (**F**) Optical microscopy image of the film after healing at 90°C for 15 min. Scale bars, 5 mm (A to C) and 20 μm (E and F).

length of 10 mm, and a strain rate of 10 mm min^{-1} were adopted. The test was repeated at least three times, and the average values were recorded. Young's modulus was determined from the initial slope of the stress-strain curves. Dynamic mechanical analysis (DMA) was conducted with TA instruments (Q800 DMA). For self-healing tests, the polymer film was crosscut and then heated at 90°C for 15 min for healing. Depth-sensing indentation measurements were performed by indentation at room temperature with a maximum depth of 1100 nm at a loading and unloading rate of 1100 nm min^{-1}. Before each measurement, a height calibration of the local sample surface was performed. Unloading curves were used to determine the elastic modulus according to the Oliver and Pharr model using CSM nanoindentation software (*56*). Contact angle and CAH measurements were carried out with OCA 20 equipment (Data Physics, Germany) under ambient conditions. To measure the CAH, the surface was tilted with respect to the horizontal plane until the liquid droplet started to slide along the surface. Then, advancing (θ_{Adv}) and receding (θ_{Rec}) contact angles were measured by a single 10-μl droplet of liquid with tilt angles of less than 10° unless otherwise specified. Each reported contact angle or CAH was an average of at least 10 independent measurements. XPS was performed with a Scanning Auger XPS (PHI5802). AFM measurements were performed on a bioscope catalyst AFM (Bruker) using Si_3N_4 tips (DNP-B, Bruker) in the PeakForce quantitative nanomechanical property mapping mode. For shear strength tests, the siloxane oligomer grind was heated to yield a viscous material, subsequently deposited onto a substrate. The deposition area was fixed as 1.00 cm^2. After the deposition, another substrate was used to hot-press the deposited siloxane oligomer material. The thickness of the supramolecular polymer between the two substrates was 0.2 mm. The shear strength tests were performed with INSTRON-5566. The two substrates adhered between two fixtures in a vertical direction. The strain rate applied was 10 mm min^{-1}, and the data were recorded in real time.

SUPPLEMENTARY MATERIALS

Supplementary material for this article is available at http://advances.sciencemag.org/cgi/content/full/5/11/eaaw5643/DC1

Fig. S1. Mechanical properties of siloxane oligomer materials with different MWs.
Fig. S2. Structures of siloxane oligomer materials with different MWs.
Fig. S3. Full ATR-IR spectra of different parts in DOSS coatings.
Fig. S4. Surface chemistry of the surface layer of DOSS coatings.

Fig. S5. Surface chemistry of the interior section of DOSS coatings.
Fig. S6. Surface chemistry of the bottom layer of DOSS coatings.
Fig. S7. Morphologies of different parts in DOSS coatings.
Fig. S8. Application of siloxane oligomer materials as adhesive materials.
Fig. S9. Oil repellency and contact angle/CAH values of DOSS coatings with different MWs.
Fig. S10. Surface chemistry of the surface layer of DOSS coatings with MW of ~3000.
Fig. S11. Surface chemistry of the surface layer of DOSS coatings with MW of ~5000.
Fig. S12. Morphologies of the surface layers in DOSS coatings with different MWs.
Fig. S13. Stability of DOSS coatings.
Fig. S14. Self-healing properties of the DOSS coatings (~870-MW siloxane oligomers) in different healing conditions.
Table S1. Mechanical properties of DOSS coatings with different MWs.
Table S2. Assignment of the feature ATR–Fourier transform infrared bands of the spectra of the surface layer, interior section, and bottom layer of DOSS coatings corresponding to Fig. 2A and fig. S3.
Table S3. Assignment of the relative atom content of the surface layer, interior section, and bottom layer of DOSS coating (MW, 870) from the corresponding XPS spectra.
Table S4. Assignment of the relative atom content of the surface layers of DOSS coatings with different MWs from the corresponding XPS spectra.

REFERENCES AND NOTES

1. S. Wang, K. Liu, X. Yao, L. Jiang, Bioinspired surfaces with superwettability: New insight on theory, design, and applications. *Chem. Rev.* **115**, 8230–8293 (2015).
2. Y. Lu, S. Sathasivam, J. Song, C. R. Crick, C. J. Carmalt, I. P. Parkin, Robust self-cleaning surfaces that function when exposed to either air or oil. *Science* **347**, 1132–1135 (2015).
3. J. Jiang, J. Gao, H. Zhang, W. He, J. Zhang, D. Daniel, X. Yao, Directional pumping of water and oil microdroplets on slippery surface. *Proc. Natl. Acad. Sci. U.S.A.* **116**, 2482–2487 (2019).
4. M. Rabnawaz, G. Liu, H. Hu, Fluorine-free anti-smudge polyurethane coatings. *Angew. Chem. Int. Ed.* **54**, 12722–12727 (2015).
5. W. He, P. Liu, J. Zhang, X. Yao, Emerging applications of bioinspired slippery surfaces in biomedical fields. *Chem. Eur. J.* **24**, 14864–14877 (2018).
6. L. Li, Y. Bai, L. Li, S. Wang, T. Zhang, A superhydrophobic smart coating for flexible and wearable sensing electronics. *Adv. Mater.* **29**, 1702517 (2017).
7. Q. Sun, B. Aguila, G. Verma, X. Liu, Z. Dai, F. Deng, X. Meng, F.-S. Xiao, S. Ma, Superhydrophobicity: Constructing homogeneous catalysts into superhydrophobic porous frameworks to protect them from hydrolytic degradation. *Chem* **1**, 628–639 (2016).
8. G. Huang, Q. Yang, Q. Xu, S.-H. Yu, H.-L. Jiang, Polydimethylsiloxane coating for a palladium/MOF composite: Highly improved catalytic performance by surface hydrophobization. *Angew. Chem. Int. Ed.* **55**, 7379–7383 (2016).
9. R. Wen, S. Xu, X. Ma, Y.-C. Lee, R. Yang, Three-dimensional superhydrophobic nanowire networks for enhancing condensation heat transfer. *Joule* **2**, 269–279 (2018).
10. T. Verho, C. Bower, P. Andrew, S. Franssila, O. Ikkala, R. H. A. Ras, Mechanically durable superhydrophobic surfaces. *Adv. Mater.* **23**, 673–678 (2011).
11. Y. Li, L. Li, J. Sun, Bioinspired self-healing superhydrophobic coatings. *Angew. Chem. Int. Ed.* **49**, 6129–6133 (2010).
12. S. Pan, R. Guo, M. Bjornmalm, J. J. Richardson, L. Li, C. Peng, N. Bertleff-Zieschang, W. Xu, J. Jiang, F. Caruso, Coatings super-repellent to ultralow surface tension liquids. *Nat. Mater.* **17**, 1040–1047 (2018).
13. L. Yu, G. Y. Chen, H. Xu, X. Liu, Substrate-independent, transparent oil-repellent coatings with self-healing and persistent easy-sliding oil repellency. *ACS Nano* **10**, 1076–1085 (2016).
14. Y. Zushi, J. N. Hogarh, S. Masunaga, Progress and perspective of perfluorinated compound risk assessment and management in various countries and institutes. *Clean Technol. Environ. Policy* **14**, 9–20 (2012).
15. T.-S. Wong, S. H. Kang, S. K. Tang, E. J. Smythe, B. D. Hatton, A. Grinthal, J. Aizenberg, Bioinspired self-repairing slippery surfaces with pressure-stable omniphobicity. *Nature* **477**, 443–447 (2011).
16. N. Vogel, R. A. Belisle, B. Hatton, T. S. Wong, J. Aizenberg, Transparency and damage tolerance of patternable omniphobic lubricated surfaces based on inverse colloidal monolayers. *Nat. Commun.* **4**, 2167 (2013).
17. Q. Wei, C. Schlaich, S. Prevost, A. Schulz, C. Bottcher, M. Gradzielski, Z. Qi, R. Haag, C. A. Schalley, Supramolecular polymers as surface coatings: Rapid fabrication of healable superhydrophobic and slippery surfaces. *Adv. Mater.* **26**, 7358–7364 (2014).
18. J. Cui, D. Daniel, A. Grinthal, K. Lin, J. Aizenberg, Dynamic polymer systems with self-regulated secretion for the control of surface properties and material healing. *Nat. Mater.* **14**, 790–795 (2015).
19. J. Zhou, P. Han, M. Liu, H. Zhou, Y. Zhang, J. Jiang, P. Liu, Y. Wei, Y. Song, X. Yao, Self-healable organogel nanocomposite with angle-independent structural colors. *Angew. Chem. Int. Ed.* **56**, 10462–10466 (2017).
20. H. Zhao, Q. Sun, X. Deng, J. Cui, Earthworm-inspired rough polymer coatings with self-replenishing lubrication for adaptive friction-reduction and antifouling surfaces. *Adv. Mater.* **30**, 1802141 (2018).
21. N. Lu, D.-H. Kim, Flexible and stretchable electronics paving the way for soft robotics. *Soft Robot.* **1**, 53–62 (2014).
22. S. H. Jeong, S. Zhang, K. Hjort, J. Hilborn, Z. Wu, PDMS-based elastomer tuned soft, stretchable, and sticky for epidermal electronics. *Adv. Mater.* **28**, 5830–5836 (2016).
23. T. Aida, E. W. Meijer, S. I. Stupp, Functional supramolecular polymers. *Science* **335**, 813–817 (2012).
24. L. Yang, X. Tan, Z. Wang, X. Zhang, Supramolecular polymers: Historical development, preparation, characterization, and functions. *Chem. Rev.* **115**, 7196–7239 (2015).
25. J.-C. Lai, J.-F. Mei, X.-Y. Jia, C.-H. Li, X.-Z. You, Z. Bao, A stiff and healable polymer based on dynamic-covalent boroxine bonds. *Adv. Mater.* **28**, 8277–8282 (2016).
26. M. Kathan, P. Kovaříček, C. Jurissek, A. Senf, A. Dallmann, A. F. Thunemann, S. Hecht, Control of imine exchange kinetics with photoswitches to modulate self-healing in polysiloxane networks by light illumination. *Angew. Chem. Int. Ed.* **55**, 13882–13886 (2016).
27. C.-H. Li, C. Wang, P. Zheng, Y. Cao, F. Lissel, C. Keplinger, C. Linder, J.-L. Zuo, L. Jin, X.-Z. You, Y. Sun, Z. Bao, A highly stretchable autonomous self-healing elastomer. *Nat. Chem.* **8**, 618–624 (2016).
28. Q. Zhang, S. Niu, L. Wang, J. Lopez, S. Chen, Y. Cai, R. Du, Y. Liu, J. C. Lai, L. Liu, C. H. Li, X. Yan, C. Liu, J. B. Tok, X. Jia, Z. Bao, An elastic autonomous self-healing capacitive sensor based on a dynamic dual crosslinked chemical system. *Adv. Mater.* **30**, 1801435 (2018).
29. J. Kang, D. Son, G.-J. N. Wang, Y. Liu, J. Lopez, Y. Kim, J. Y. Oh, T. Katsumata, J. Mun, Y. Lee, L. Jin, J. B.-H. Tok, Z. Bao, Tough and water-insensitive self-healing elastomer for robust electronic skin. *Adv. Mater.* **30**, 1706846 (2018).
30. G. M. Whitesides, Soft robotics. *Angew. Chem. Int. Ed.* **57**, 4258–4273 (2018).
31. M. Liu, P. Liu, G. Lu, Z. Xu, X. Yao, Multiphase-assembly of siloxane oligomers with improved mechanical strength and water-enhanced healing. *Angew. Chem. Int. Ed.* **57**, 11242–11246 (2018).
32. Q. Zhang, C.-Y. Shi, D.-H. Qu, Y.-T. Long, B. L. Feringa, H. Tian, Exploring a naturally tailored small molecule for stretchable, self-healing, and adhesive supramolecular polymers. *Sci. Adv.* **4**, eaat8192 (2018).
33. D. W. R. Balkenende, C. A. Monnier, G. L. Fiore, C. Weder, Optically responsive supramolecular polymer glasses. *Nat. Commun.* **7**, 10995 (2016).
34. D. J. M. van Beek, A. J. H. Spiering, G. W. M. Peters, K. te Nijenhuis, R. P. Sijbesma, Unidirectional dimerization and stacking of ureidopyrimidinone end groups in polycaprolactone supramolecular polymers. *Macromolecules* **40**, 8464–8475 (2007).
35. D. Alsteens, R. Newton, R. Schubert, D. Martinez-Martin, M. Delguste, B. Roska, D. J. Müller, Nanomechanical mapping of first binding steps of a virus to animal cells. *Nat. Nanotechnol.* **12**, 177–183 (2017).
36. D. F. Cheng, C. Urata, M. Yagihashi, A. Hozumi, A statically oleophilic but dynamically oleophobic smooth nonperfluorinated surface. *Angew. Chem. Int. Ed.* **51**, 2956–2959 (2012).
37. J. P. Rolland, R. M. V. Dam, D. A. Schorzman, S. R. Quake, J. M. DeSimone, Solvent-resistant photocurable "liquid teflon" for microfluidic device fabrication. *J. Am. Chem. Soc.* **126**, 2322–2323 (2004).
38. L. Wang, T. J. McCarthy, Covalently attached liquids: Instant omniphobic surfaces with unprecedented repellency. *Angew. Chem. Int. Ed.* **55**, 244–248 (2016).
39. P. Liu, H. Zhang, W. He, H. Li, J. Jiang, M. Liu, H. Sun, M. He, J. Cui, L. Jiang, X. Yao, Development of "liquid-like" copolymer nanocoatings for reactive oil-repellent surface. *ACS Nano* **11**, 2248–2256 (2017).
40. S. Wooh, N. Encinas, D. Vollmer, H.-J. Butt, Stable hydrophobic metal-oxide photocatalysts via grafting polydimethylsiloxane brush. *Adv. Mater.* **29**, 1604637 (2017).
41. R. Wang, T. Xie, Macroscopic evidence of strong cation-pi interactions in a synthetic polymer system. *Chem. Commun.* **46**, 1341–1343 (2010).
42. Y. Ahn, Y. Jang, N. Selvapalam, G. Yun, K. Kim, Supramolecular velcro for reversible underwater adhesion. *Angew. Chem. Int. Ed.* **52**, 3140–3144 (2013).
43. W. Wang, Y. Xu, A. Li, T. Li, M. Liu, R. von Klitzing, C. K. Ober, A. B. Kayitmazer, L. Li, X. Guo, Zinc induced polyelectrolyte coacervate bioadhesive and its transition to a self-healing hydrogel. *RSC Adv.* **5**, 66871–66878 (2015).
44. T. Kakuta, Y. Takashima, T. Sano, T. Nakamura, Y. Kobayashi, H. Yamaguchi, A. Harada, Adhesion between semihard polymer materials containing cyclodextrin and adamantane based on host–guest interactions. *Macromolecules* **48**, 732–738 (2015).
45. C. Heinzmann, U. Salz, N. Moszner, G. L. Fiore, C. Weder, Supramolecular cross-links in poly(alkyl methacrylate) copolymers and their impact on the mechanical and reversible adhesive properties. *ACS Appl. Mater. Interfaces* **7**, 13395–13404 (2015).
46. S. Dong, J. Leng, Y. Feng, M. Liu, C. J. Stackhouse, A. Schönhals, L. Chiappisi, L. Gao, W. Chen, J. Shang, L. Jin, Z. Qi, C. A. Schalley, Structural water as an essential comonomer in supramolecular polymerization. *Sci. Adv.* **3**, eaao0900 (2017).
47. J. Yang, R. Bai, Z. Suo, Topological adhesion of wet materials. *Adv. Mater.* **30**, 1800671 (2018).

48. A. H. Hofman, I. A. van Hees, J. Yang, M. Kamperman, Bioinspired underwater adhesives by using the supramolecular toolbox. *Adv. Mater.* **30**, 1704640 (2018).
49. J.-C. Lai, L. Li, D.-P. Wang, M.-H. Zhang, S.-R. Mo, X. Wang, K.-Y. Zeng, C.-H. Li, Q. Jiang, X.-Z. You, J.-L. Zuo, A rigid and healable polymer cross-linked by weak but abundant Zn(II)-carboxylate interactions. *Nat. Commun.* **9**, 2725 (2018).
50. C. Cui, T. Wu, F. Gao, C. Fan, Z. Xu, H. Wang, B. Liu, W. Liu, An autolytic high strength instant adhesive hydrogel for emergency self-rescue. *Adv. Funct. Mater.* **28**, 1804925 (2018).
51. G. Ju, M. Cheng, F. Guo, Q. Zhang, F. Shi, Elasticity-dependent fast underwater adhesion demonstrated by macroscopic supramolecular assembly. *Angew. Chem. Int. Ed.* **57**, 8963–8967 (2018).
52. M. A. Eddings, M. A. Johnson, B. K. Gale, Determining the optimal PDMS–PDMS bonding technique for microfluidic devices. *J. Micromech. Microeng.* **18**, 067001 (2008).
53. X. Yao, Y. Hu, A. Grinthal, T.-S. Wong, L. Mahadevan, J. Aizenberg, Adaptive fluid-infused porous films with tunable transparency and wettability. *Nat. Mater.* **12**, 529–534 (2013).
54. J. N. Lee, C. Park, G. M. Whitesides, Solvent compatibility of poly(dimethylsiloxane)-based microfluidic devices. *Anal. Chem.* **75**, 6544–6554 (2003).
55. C. Urata, B. Masheder, D. F. Cheng, D. F. Miranda, G. J. Dunderdale, T. Miyamae, A. Hozumi, Why can organic liquids move easily on smooth alkyl-terminated surfaces? *Langmuir* **30**, 4049–4055 (2014).
56. W. C. Oliver, G. M. Pharr, Measurement of hardness and elastic modulus by instrumented indentation: Advances in understanding and refinements to methodology. *J. Mater. Res.* **19**, 3–20 (2004).

Acknowledgments
Funding: We acknowledge project funding provided by the National Natural Science Foundation of China (grant no. 21501145), the General Research Fund (GRF) Hong Kong (CityU 11274616), and the Collaborative Research Fund (CRF) Hong Kong (grant no. C1018-17G). **Author contributions:** X.Y. conceived the idea and led the project. X.Y. and M.L. designed the experiments. M.L. synthesized and fabricated the samples and performed characterization. Zhaoyue Wang, P.L., and Zuankai Wang supported the imaging processes. H.Y. supported the tensile test and indentation measurement processes. M.L. and X.Y. wrote the paper. All authors discussed the results and commented on the manuscript. **Competing interests:** The authors declare that they have no competing interests. **Data and materials availability:** All data needed to evaluate the conclusions in the paper are present in the paper and/or the Supplementary Materials. Additional data related to this paper may be requested from the authors.

Submitted 5 February 2019
Accepted 16 September 2019
Published 1 November 2019
10.1126/sciadv.aaw5643

Citation: M. Liu, Z. Wang, P. Liu, Z. Wang, H. Yao, X. Yao, Supramolecular silicone coating capable of strong substrate bonding, readily damage healing, and easy oil sliding. *Sci. Adv.* **5**, eaaw5643 (2019).